EUROPEAN COOPERATION
IN THE FIELD OF SCIENTIFIC
AND TECHNICAL RESEARCH

EURO-COST

IC1004 TD(12)04025
Lyon, France
3-4 May, 2012

SOURCE: Comelec Department,
Telecom ParisTech,
France

Comparative assessment of antenna mode and clutter signals in backscattering based UWB-RFID detection

R. Contreras and A.Sibille
Télécom ParisTech
46 rue Barrault
75634 Paris cedex 13
FRANCE
Phone: + 33-1 45 81 70 60
Fax: + 33-1 45 80 40 36
Email: (contrera,Alain.Sibille) @telecom-paristech.fr

Comparative assessment of antenna mode and clutter signals in backscattering based UWB-RFID detection

Richard Contreras and Alain Sibille

TELECOM-ParisTech and ENSTA-ParisTech

E-mail: contrera@telecom-paristech.fr

***Abstract*—In modulated backscattering based RFID systems, the "antenna mode" signal received by the reader from the tag can be strongly masked by that originating from the environment (clutter). Although differential detection and appropriate coding may mitigate this problem, it is important to quantitatively evaluate the respective magnitude of both signals. In that work this has been done for a UWB RFID system, intended to operate in the 3-5 GHz band. From 5 ports channel measurements between a set of 4 reader antennas and a tag antenna in various orientations, the antenna mode signal and the clutter signal in the same time window have been determined over a grid of tag positions, providing a distance-dependent statistical model of the signal to clutter power ratio.**

Keywords-component; formatting; style; styling; insert (key words)

I. INTRODUCTION

A. UWB RFID system description

It is well known that RFID systems are rapidly penetrating the commercial and industrial sectors, as a way the incorporate things into the digital world. Among RFIDs, Ultra Wide Band (UWB) systems have unique advantages, mainly the capability of high localization accuracy and the low power consumption (both on tag and in the readers). The SELECT european project [1] aims at developing such a system, where rather than using a fully active transponder, a modulated backscattering (BS) principle is adopted. The on-tag power consumption is very small, since there is no transmitter but only an impedance load switching mechanism activated during the detection and localization protocol.

Although the idea of modulated BS is very attractive, it faces many technical challenges. One is the very low scattered power, which requires mitigation through proper energy integration and coding techniques. Another, related, is the fact that the signal backscattered by the environment (clutter) is usually much larger than that backscattered by the tag, again requiring appropriate mitigation techniques. Therefore, in this work we address the experimental investigation of compared tag and environment backscattering. The goal is dual: i) determine the distance dependent useful (i.e. antenna mode) backscattered tag signal and ii) determine the total magnitude of the clutter power and also the clutter power falling into the time window where the antenna mode tag BS signal is detected.

B. UWB RFID Tag Backscattering

The signal backscattered by the tag is composed of two contributions, which are the structural and the antenna mode scattering[2][3]. We here define the structural mode as the one when the antenna is loaded with the reference impedance (50 Ohms). The structural mode BS is dominated by the physical structuring of the antenna parts (even including its support, connecter...) and is not directly related to its radiation/transmission characteristics. On the other hand, the antenna mode expresses that when the load connected to the tag differs from the reference impedance, the received signal is partly or totally reflected by this load and reradiated. In other words, the antenna ordinary radiation characteristics are involved twice in antenna mode BS: in reception and in transmission sequentially.

It can be shown that the bistatic tag scattering can be written as follows:

$$H^B_{tag} = H^B_{tag-match} + H^B_{tag-ant} \tag{1}$$

where the first term expresses the structural mode and the second is the antenna mode. H^B_{tag} is the bistatic backscattering transfer function (dimensionless) and is defined by:

$$H^B_{tag} = \frac{4\pi r}{\lambda} \frac{E^{FF}_{sc} \cdot e^{jkr}}{E^{FF}_{inc}} \tag{2}$$

where E^{FF}_{sc} is the far field scattered complex spherical wave amplitude (hence the scattering distance *r* in the numerator) and E^{FF}_{inc} is the incident complex plane wave amplitude. It can be easily shown that in the antenna mode:

$$H^B_{tag-ant}(\Omega_{inc},\Omega_{sc}) = -jH^T_{tag-ant}(\Omega_{inc}) \cdot H^T_{tag-ant}(\Omega_{sc}) \cdot \frac{\Gamma_L}{1-S_{22}\Gamma_L} \tag{3}$$

where $H^T_{tag-ant}$ is the ordinary (dimensionless) tag antenna transfer function in transmission (equal to 1 for a lossless isotropic antenna), and $(\Omega_{inc},\Omega_{sc})$ express the incident and scattered waves directions. Γ_L and S_{22} are, respectively, the load impedance and the tag antenna reflection coefficient. It is obvious that when the load is equal to the reference impedance, the antenna mode contribution disappears.

In the following, we will assume that the tag antenna has been properly designed, so that its internal impedance equals 50 Ohms, so that $S_{22} = 0$. In practice, with the antennas used in the described measurements, this is close to reality.

In evaluating the tag antenna mode BS signal, we first observe that eq. (3) applies to any incoming and outgoing direction, thus it lends itself readily to incorporation in a full multipath backscattering channel model, as presented in [4]. Secondly, we see from eqs. (1) and (3) that the antenna mode can be isolated, and maximized, by measuring the difference between the BS signals for an open $\Gamma_L = +1$ and a short circuited $\Gamma_L = -1$ tag antenna. If $S_{22} = 0$, the difference equals $-2jH^T_{tag-ant}(\Omega_{inc}) \cdot H^T_{tag-ant}(\Omega_{sc})$, in other words, both the structural and the clutter signals are cancelled through differential detection. Unfortunately, this implies a perfect cancellation of the latter signals, thus an infinite measuring dynamic range and perfectly static signals, which may not always be respected, hence the reason for the present work.

C. *Antenna mode backscattering from one way channel measurements.*

In last section it has been verified that measurements in one way channel provide the antenna mode scattering by assuming ideal conditions of open-short loads and a perfectly matched tag antenna. Some advantages are that, a single measurement provides better reliability, is less time consuming and is easier to measure than two way backscattering channel in terms of signal-to-noise ratio.

In this work we are only interested in characterizing the antenna mode which corresponds:

$$H_{BS}(f) = -2jH^T_{tag-ant}(\Omega_{inc}) \cdot H^T_{tag-ant}(\Omega_{sc}) \quad (4)$$

The antenna mode backscattering is contained in the rough channel impulse response of a UWB-RFID system, which can be expressed:

$$F^{-1}\{H_{xy}(f)\} = h_{MC}(\tau) + h_C(\tau) + h_{BS_S}(\tau) + h_{BS_L}(\tau) \quad (5)$$

Where, $h_{MC}(\tau)$ is the mutual coupling, $h_C(\tau)$ represent the clutter and $h_{BS_S}(\tau), h_{BS_L}(\tau)$ are the structural and the antenna mode backscattering.

Nevertheless, we will focus on the channel backscattering impulse response i.e.:$\mathrm{CIR_{BS}}(\tau) = F^{-1}\{H_{BS}(f)\}$

Or equivalently the power delay profile (PDP) i.e.: $|CIR_{BS}(\tau)|^2$

In addition, we can easily obtain the ratio of the received power to the transmit power which is a parameter called the path gain; it determines the average signal-to-noise ratio (SNR) and in our case study also the signal to clutter ratio (SCR).

D. *Clutter*

The clutter is not a useful signal that can be exploited, and it can strongly disturb the UWB-RFID backscattering system, as mentioned above. This depends on the number and size of scatterers, on the size of the room and on the antenna radiation properties, among others. Thus, the UWB-RFID systems require clutter suppression capabilities, as presented in [5] and investigated in SELECT [1].

The clutter signals received by the reader thus come from various places of the environment and arrive at varying delays, from very short ones for close objects to long ones, due to e.g. far walls or pieces of furniture. In the operation of the reader, we should distinguish between the total clutter energy in the backscattered impulse response, which may e.g. saturate the first receiver stage, from the clutter signal in the time window selected for the detection of the targeted tag. These two quantities will, therefore, be investigated in the measurements below.

Figure 1. Pictures of room E200.

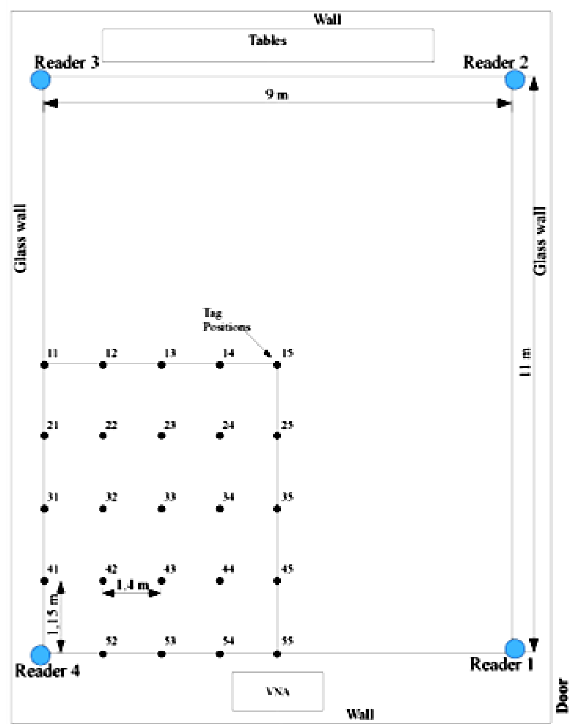

Figure 2. Room E-200 and grid of 24 positions.

II. MEASUREMENT SETUP AND ENVIRONMENT

A. *Scenario and environment*

The UWB backscattering channel measurement campaign has been carried out in a large room (E200, see Figure 1.). This case is considered to be a reference scenario for the SELECT project, where the clutter is not considered to be a worst case scenario. Further works will consider a warehouse scenario, which is a representative scenario of some of the large number of UWB-RFID applications. In the measured E200 scenario, the room was basically empty and the scatterers, such as tables and wood closets were located along the walls. A major feature was that the two main side walls were made of glass, the other side being the building outside. Among important scatterers were metallic poles on the whole room height and two metallic doors. Four metallic tripods which were also used as supports of each reader antenna.

The whole set of reader antennas and tag antennas positions is shown in Figure 2. The readers are located at the 4 corners of a rectangle of sides 9 m and 11 m. On account of the gross symmetry of the scenario, the tag antenna positions ahev been take to be a grid of 25-1=24 positions, covering a quarter of the whole rectangle. The measuring system was put on a table on one side of the room, outside the rectangle.

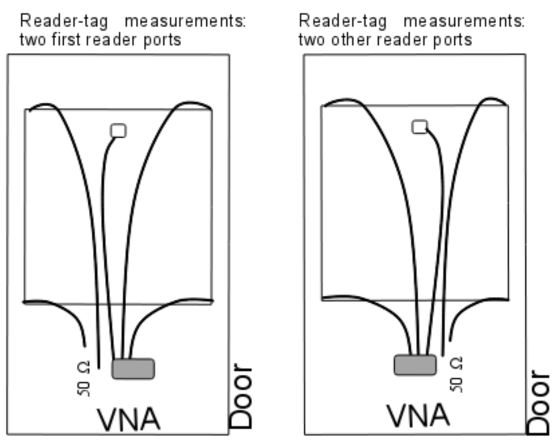

Figure 3. *Reader-Tag measurements.*

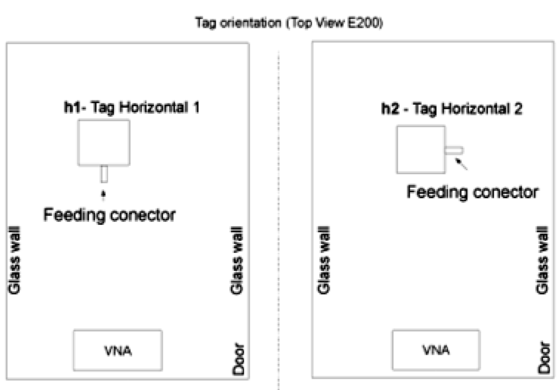

Figure 4. Horizontal Tag orientations.

B. Measurement setup and parameters

The measurements have been performed in the frequency domain by measuring the full [S] parameters of the radio channel by using an AGILENT ENA 5071C four ports Vector Network Analyzer (VNA) fully calibrated at connector level for all antennas. In these measurements we wished to obtain:

- the reflection coefficient of each tag and reader antenna
- the transmission coefficient between all pairs of reader antennas
- the transmission coefficient between the tag and each reader antenna

This makes a total of 15 independent coefficients, i.e. the whole 5 ports [S] matrix, given reciprocity. In practice, since only a 4-ports VNA was available, in addition to measuring once the [S] matrix for the 4 reader antennas, this was done by measuring for each tag position two successive 3-ports configuration, as shown in Figure 3.

We set the frequency bandwidth from 2 to 6 GHz with a step size of 2.5 MHz. However in this work we consider only the band 3-5 GHz, which is the retained one for the SELECT system design.

The measurements were carried out in room E-200 of Telecom-ParisTECH. The tag was moved manually over the 24 positions mentioned above, arranged over a 4.6m x 5.6m rectangle grid with 1.15m x 1.40 m spacing. The reader antennas were located at 2m height from ground and the tag antenna at 1.12m height from ground. The cables used to connect the tag and the reader antennas to the VNA were high quality "constant phase" cables. Finally, in order to avoid any perturbation during the measurements, it was ensured that no people were moving around.

C. Reader and Tag antennas

Four different sorts of UWB antennas were implemented in our measurements. For the reader antennas, we tried two kinds:

- a bicone, of excellent omnidirectionality and good stability in elevation over the band width
- a planar balance dipole (PBD), which is moderately directional

Both antennas have been designed to operate in the band 2.3-12 GHz.

For the tag antenna we used the DFMS and DFMM described below:

- The DFMS (dual feed monopole stripline) is basically a planar dipole, vertically polarized with a symmetry plane. The radiation is essentially omnidirectional around the vertical axis, however due to its planarity the gain tends to be smaller in the plane than normally to it.
- The DFMM (dual feed monopole microstrip) antenna operates according to the same general principle as the DFMS, however instead of feeding by a stripline, it is achieved through a microstrip waveguide. This effectively introduces some differences in the radiation patterns, compared to the DFMS.

The reader antennas were always vertically polarized (in both PBD and bicone cases). On the other hand, the tag antenna was oriented in three different positions, vertically with the ground plane oriented toward the VNA and horizontally with two different orientations as shown in Figure 4.

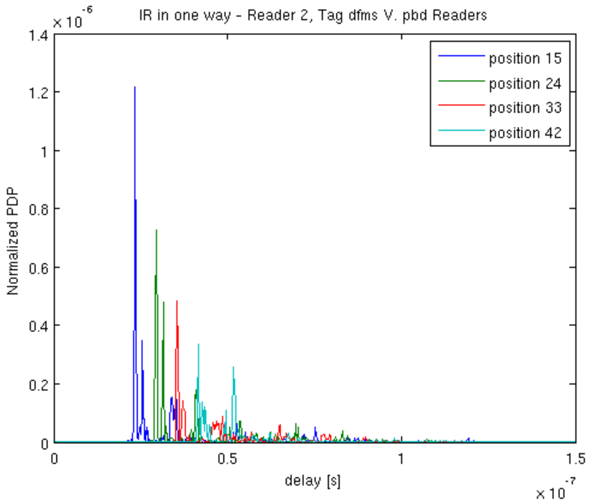

Figure 5. one-way PDP seen by reader 2 for several tag positions

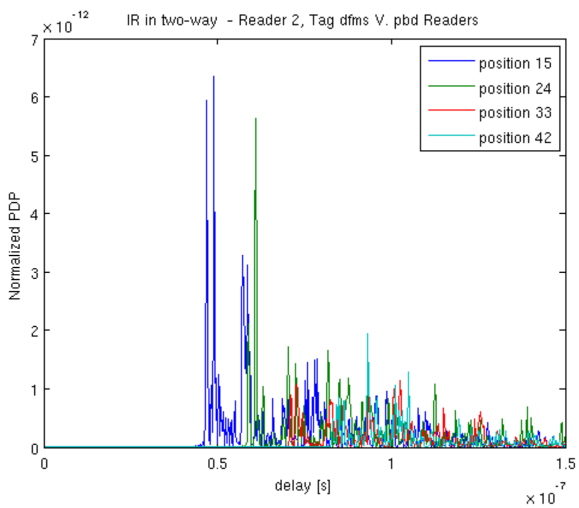

Figure 6. backscattering PDP seen by reader 2 for several tag positions .

III. DATA PROCESSING AND MODELLING

A. One-way and two-way Impulse response

The "one-way" frequency domain transmission coefficient $T_{xy}(f)$ between the tag and reader is readily obtained as the corresponding S_{xy} parameter. The one way impulse response $\mathrm{h(t)}$ was computed after zero padding over the zero centered domain and hamming windowing over the band [3-5] GHz, followed by inverse Fourier transform (IFFT). The power delay profile (PDP) is subsequently obtained as the magnitude squared of the impulse response: $PDP = |h(t)|^2$. In the results presented below, we systematically normalized the PDP to a reference PDP computed in the same way, with 1 instead S_{xy}. An example of such one-way PDPs between a reader and a tag in several positions is shown in Figure 5.

According to section I.B, the two-way BS signal is computed from the one-way transmission between a reader and the tag through the formula $BS = 2 * T(f)_{xy}^2$, assuming ideal open-short impedance switching and a perfectly matched tag antenna. An example of such two-way PDPs seen by the readers for several positions of the tag is shown in Figure 6. We can notice the doubling of the propagation delay and the higher richness of the PDP in the BS case. Both can be explained by the fact that the two-way BS signal is due to the square of the one-way frequency domain transmission, which also means that the BS impulse response is the one-way IR convoluted by itself.

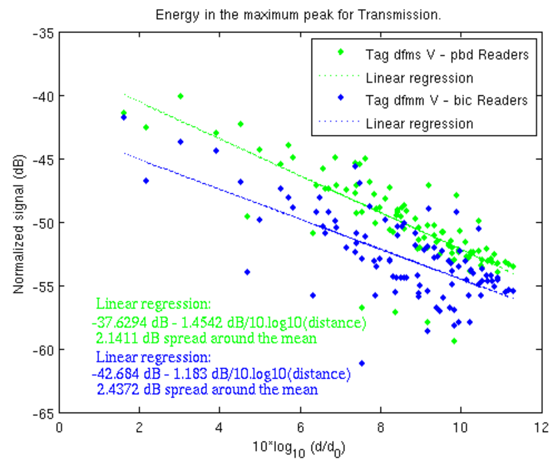

Figure 7. One way IR. Energy contained in the maximum peak for DFMM and DFMS tags vertically oriented with PBD and bicone readers.

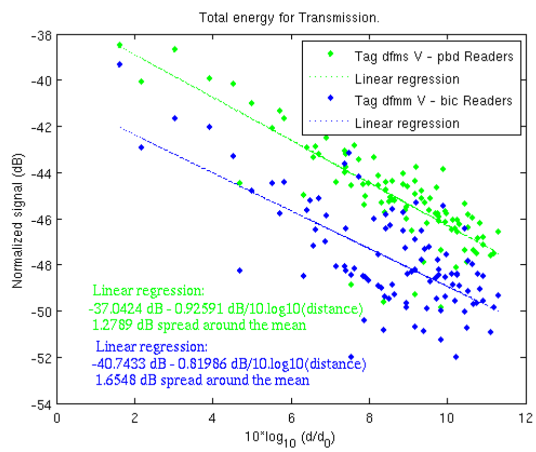

Figure 8. One way IR. Total energy for DFMM and DFMS tags vertically oriented with PBD and bicone readers.

B. Distance dependent path gain modeling

The grid of tag positions is shown in Figure 2. It allows to extract a path gain exponent by computing a linear regression of the PDP in dB vs the logarithm of the distance (referenced to 1 m), as expressed below:

$$\overline{\mathrm{G}}|_{\mathrm{dB}} = -\mathrm{n} * 10 * \log_{10}\left(\frac{\mathrm{d}}{\mathrm{d_0}}\right) + \mathrm{G_0} \qquad (6)$$

Where G_0 is the channel gain at the reference distance d_0, and n is the path gain exponent. In the analysis, we will distinguish between the energy contained in the highest peak of the PDP, integrated over a 2 ns duration, vs. the total energy integrated over the whole PDP. The former is probably more relevant from a system point of view, corresponding to a single rake finger, while the latter would be relevant for an "all-fingers" rake receiver, which is basically impossible to achieve. The model of eq. (6) will help us also in the assessment of the two-way response.

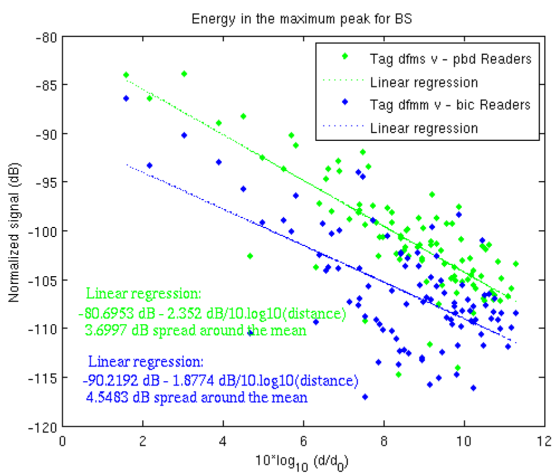

Figure 9. Two-way IR. Energy contained in the highest peak for DFMM and DFMS tags vertically oriented, with PBD and bicone readers.

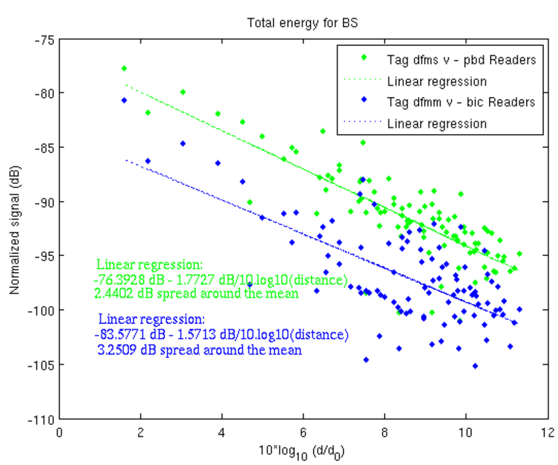

Figure 10. Two-way IR. Total energy for DFMM and DFMS tags vertically oriented, with PBD and bicone readers.

The data points and the regression for the tags vertically oriented, with either the PBD or the bicones as readers, are presented in Figure 7. and Figure 8. In a free space scenario we expect a path gain exponent approximately of 2, since the attenuation increases with the square of the distance. Nevertheless, calculating the energy contained in the maximum peak (also over 2ns), we find different values of n for the case of the two different sorts of readers, obtaining n=1.45 for the PBD readers and n=1.18 for the bicone readers. This can be due to the fact that in some positions where the tag is closest to the reader, the angular inclination between the tag and the reader antennas is highest than in far positions, and the radiation pattern of the directional PBD antennas might not cover adequately the tag. It is also possible that the radiation pattern of the tag antennas influence the difference in the path gain exponent, since the DFMM tag radiation pattern over the band 3-5 GHz presents a difference of approximately 6 dB in the opposite side of the ground plane. This means that readers 2 and 3 will receive a power different from readers 1 and 4 at the same distance, given the tag orientation used.

On the other hand, we have found that the path gain exponents for the total energy in transmission are quite similar, which is due to the consideration of the totality of all multipath components arriving over all tag positions. The gap between the PBD-DFMS case and the BIC-DFMM is around 4dB, probably due to the gain of the PBD antennas.

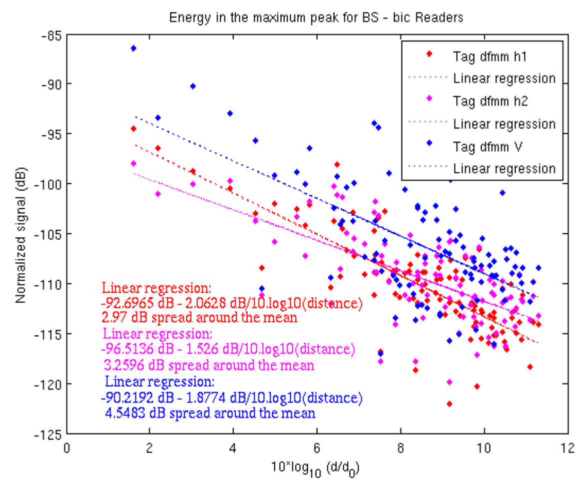

Figure 11. Two-way IR. Energy contained in the highest peak for different orientations of the DFMM tag and for bicone readers.

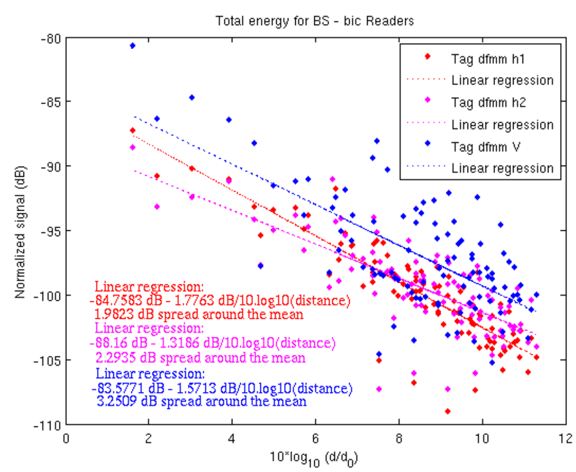

Figure 12. Two-way IR. Total energy for different orientations of DFMM tag and bicone readers.

We now analyze the two-way distance dependent path gain, and compute the linear regression in order to calculate the path gain exponent, which is expected to be twice the "one-way" channel. However this is an intuitive but incomplete view, since the maximum peak of energy in the two-way channel is not necessarily the direct path and in addition it does not necessarily coincide with the main peak of the one-way IR at a doubled delay. Below, we present the energy contained in the highest peak, and the total energy in the case where the tag is vertically oriented with different readers (Figure 9. and Figure 10.), and in the case where the tag is either vertically or horizontally oriented, in the latter case for both h1 and h2 orientations as depicted in Figure 4. (bicone readers, see Figure 11. Figure 12.).

With the purpose of easily comparing the path gain exponent "n" obtained in each case, we present in 0a summary of the results for the energy contained in the maximum peak and in TABLE II. the results for the total energy.

TABLE I. ENERGY CONTAINED IN THE HIGHEST PEAK

Reader	**Tag**	**Orientation**	**n**
BIC	DFMM	H1	2.06
		H2	1.53
		Vertical	1.89
PBD	DFMS	Vertical	2.35

TABLE II. TOTAL ENERGY

Reader	**Tag**	**Orientation**	**n**
BIC	DFMM	H1	1.78
		H2	1.32
		Vertical	1.57
PBD	DFMS	Vertical	1.78

The path gain exponents obtained in the two-way channel are somewhat different from the factor 2 higher than the one-way channel, expected for a doubled distance BS channel. The reasons for this observation are not fully clear, as many factors can be involved. The radiation pattern of both reader and tag antennas obviously affects the angular properties of the channel, and as said before the highest peak is not always the direct path.

We can observe in Figure 11. and Figure 12. that the two responses for the tag horizontally oriented perpendicular to each other and at medium and large distances have a similar behavior, but this depends on the position of the tag, since the orientation does change, relatively to each reader.

In contrast, the vertically oriented tags reach a higher signal level, but this also depends on the kind of reader implemented (directional/omnidirectional), where directional ones might have a better behavior then omnidirectional ones if the angular inclination between the tag and the readers does not change too much with the tag position.

C. Clutter and signal to clutter ratio

The same processing as in subsection I.A have been carried out in order to obtain the clutter impulse response. However, we have to take into account that the [S] parameters measured by the VNA is dominated by the antenna reflection coefficient, given that perfect matching is impossible. Fortunately, the antenna reflection occurs at extremely small delays (the first few nanoseconds) as compared to the clutter, which allows to get rid of it through a simple time gating.

As recalled above, the clutter signal originates from the reflection and other scattering events experienced by waves before they eventually returned to the antenna. Consequently, the clutter signals occur at nearly all possible delays, with a mean power tending to decrease with the delay, since delay means propagation distance. In the figures below, we compare the magnitude of the antenna mode BS signal from the tag to the clutter signal, also integrated over a 2 ns window at the same time instant. This " signal to clutter ratio" (SCR) is obviously an important parameter for the capability of the RFID system to detect a tag in a real environment where clutter signal is important. In Figure 1. is shown the time windowed clutter power vs. the tag-reader distance, for both the PBD and bicone reader antennas. We see that the clutter power seen by the PBD readers is somewhat stronger than the clutter power seen by the bicone readers. The likely reason is because of the higher gain of the PBD antennas as compared to the bicones.

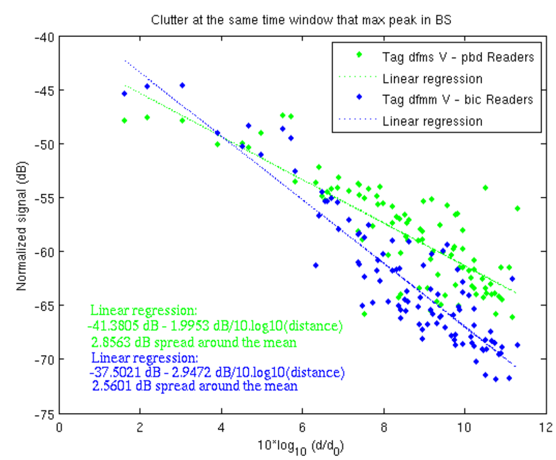

Figure 13. Clutter seen by PBD and bicone readers at the same time window that the maximum peak is presented in BS.

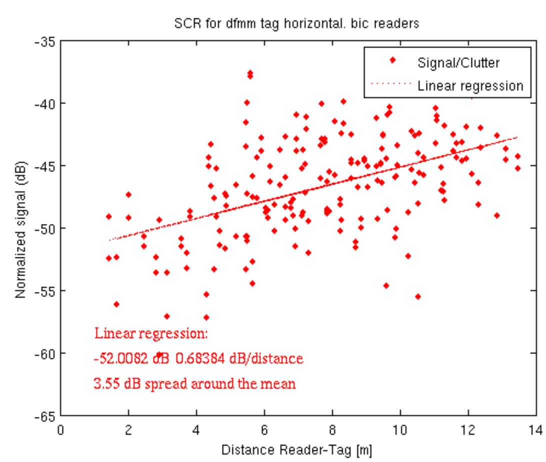

Figure 14. SCR for DFMM tag horizontal with bicone readers.

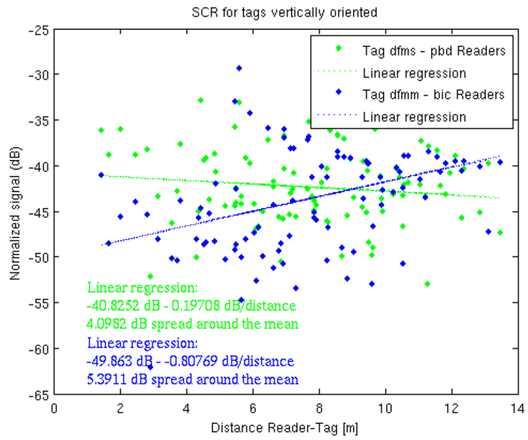

Figure 15. SCR for vertically oriented tags

The SCR is plotted in Figure 14. for the horizontal tags (both h1 and h2 orientations together, since their contribution are quite similar). In Figure 15. we compare the SCR for the vertically oriented tag, with either the PBD or the bicone reader antennas. We see that, although the clutter seen by the PBD readers is higher than for the bicone readers, the SCR is also better for the PBD antennas. This is easy to understand, since the BS signal as well as the clutter are affected by the gain of the directional PBD antennas.

We also verify, by comparing Figure 14. and Figure 15. that the SCR when the tag antennas are vertically positioned is better than that when tag antennas are horizontally oriented, since the SCR for the vertical case remains around -30 dB whereas SCR for the horizontal case remains 10 dB below, by around -40 dB.

IV. Conclusion

In this work we have shown experimental results about the one-way and two-way propagation between a set of 4 reader antennas and a tag, as a simple scenario for a UWB-RFID system based on modulated backscattering. Both the path loss and the time windowed clutter signal have been modeled vs. the reader-tag distance. The path loss exponents are, generally speaking, lower than expected.

Acknowledgment

The authors are grateful to Xin Zeng, Valerio Casadei and Moussa Sacko for their help in the measurement campaign. The research leading to these results has received funding from the European Union Seventh Framework Programme FP7/2007-2013 under grant agreement n° 257544.

References

[1] see http://www.selectwireless.eu

[2] F. Guidi, M. Sacko, A. Sibille and C. Roblin, “Analysis of UWB RFID Tag Backscattering in the Presence of Scatterers”, General Assembly and Scientific Symposium, 2011 XXXth URSI, 13-20Aug. Istanbul 2011.

[3] SELECT deliverable D2.1.1 "Backscatter propagation modelling for WP2", 28/01/2012

[4] Z. Mhanna and A. Sibille, "A Statistical UWB-RFID Backscattering Channel Model incorporating Propagation and Tag Variability", TD(12) 4012, 4th IC1004 COST meeting, May 3-4, 2012, Lyon, France

[5] Gerald Rode Site Specific Radar Clutter Backscattering Simulation Frequenz, vol. 1-2, no. 62, 2008. Fachverlag Schiele & Schön.

.